Transcriptomic Analysis and Computational Study Provide Insights into the Mechanism of Anti-tumor Activity of CuB and CuE on HepG2 cells

Ru CHEN[△], Wuyi BAN[△], Shitong SONG, Haoran MA, Yuxin ZHENG, Lei SONG[*]

College of Pharmacy, Southwest Minzu University, Chengdu 610225, China

Abstract [**Objectives**] To study the effect of carcinoma cell line (HepG2) and mechanism of anti-tumor activity of cucurbitacin B (CuB) and cucurbitacin E (CuE) on HepG2 cells. [**Methods**] HepG2 cells were treated with various concentrations of CuB and CuE, and the proliferation, cell cycle distribution, apoptosis, and performed RNA-seqtranscriptomics of these cells were evaluated after treatment. [**Results**] The results demonstrated that, in comparison to the control group, HepG2 cells treated with CuB and CuE displayed a synergistic effect on growth inhibition, cell cycle arrest at the G_2/M phase, and apoptosis induction in a concentration- and time-dependent manner. Western blotting analysis using protein extracts derived from HepG2 cells showed that CuB and CuE induced apoptosis by increasing the expression of endogenous levels of full-length caspase-3 (35 kDa) and the large fragment of cleaved caspase-3 (17 kDa). Moreover, transcriptomic results demonstrated that after treatment, the differentially expressed genes associated with pathways such as "cell cycle", "spliceosome", "metabolic pathways", and "carbon metabolism" were significantly up-/down-regulated. [**Conclusions**] These results demonstrate that the anti-tumor mechanisms of CuB and CuE are attributed to their interference in cell cycle and metabolism processes. Collectively, the treatment with CuB and CuE may serve as a promising therapeutic option for hepatocellular carcinoma.

Key words Transcriptomic, Cucurbitacin B, Cucurbitacin E, HepG2 cells

1 Introduction

Hepatocellular carcinoma (HCC) is the most common type of liver cancer with a five-year survival rate of less than 5%, and it is the fourth leading cause of cancer-related mortality in people with cirrhosis[1]. The majority of HCC cases occur in Africa and Asia, with more than half of the patients identified in China. Surgical intervention remains the preferred treatment option for early-stage HCC. However, because of the presence of cirrhosis and the multifocal nature of the disease, less than 20% of HCC patients are eligible for surgical resection[2]. Moreover, given the complexity of HCC, therapeutic strategies should be tailored to the specific characteristics of each individual patient. Chemotherapy is an alternative strategy for the treatment of unresectable tumors. Sorafenib, a tyrosine kinase inhibitor, has received approval from the Food and Drug Administration (FDA) for the management of unresectable HCC and is recommended as the first-line therapy for HCC patients[3]. Although sorafenib shows a respectable effect on the survival of patients with advanced HCC, the response to sorafenib is relatively modest, with a median overall survival extension of only 2.8 months[4]. Thus, HCC remains an unmet medical need.

There is a growing interest in the use of herbs as a potent source of novel therapeutic agents for cancer treatment. Plants are known to contain a wide variety of chemicals that exhibit potent biological effects, including anti-cancer activity[5]. Cucurbitacins are classified as highly oxygenated natural triterpenes that have been isolated from various plant families such as Cucurbitaceae. These compounds are characterized by their bitter taste and purgative properties. Numerous pharmacological studies have shown the wide range of biological activities exhibited by these compounds, including anti-inflammatory, hepatoprotective, and anti-HIV properties[6-8]. They are also extensively studied for their cytotoxic and antitumor effects against various cancer cell lines[9]. Cucurbitacin B (CuB) is one of the most abundant forms of cucurbitacins and has attracted considerable attention for its potential application in cancer therapy[10-11]. Cucurbitacin E (CuE), a widely investigated cucurbitacin, has been shown to inhibit the proliferation of cancer cells by inducing apoptosis[12] and autophagy[13], as well as causing damage to the cytoskeleton[14] in a panel of cancer cells.

The human hepatic cell line HepG2 is frequently used in the fields of toxicology and pharmacology. HepG2 cells are able to overexpress various drug-metabolizing enzymes, including those involved in Phase I and II metabolism, especially after the exposure to toxins[15-20]. Additionally, transcriptomic analysis of HepG2 has confirmed the activation of biotransformation pathways at baseline levels[21].

The purpose of the present study was to examine the effects of CuB and CuE at various concentrations on HepG2 cells, specifically focusing on cellular growth, cell-cycle distribution, apoptosis, autophagy and transcriptomes by means of Illumina sequencing technology. The results from this study not only dissect the potential molecular mechanisms underlying the anti-proliferation, apoptosis and autophagy, but also contribute to the development of bioassays to evaluate the effects of CuB and CuE.

Received: November 28, 2024 Accepted: January 22, 2025

△These authors contributed equally to this work.

Ru CHEN, master, research fields: ethnopharmacy; Wuyi BAN, master, research fields: ethnopharmacy.

* Corresponding author. Lei SONG, PhD., experimentalist, research fields: ethnopharmacy.

2 Materials and methods

2.1 Cell culture and chemicals Human hepatocellular carcinoma cell line (HepG2) was purchased from the Cell Bank of the Chinese Academy of Sciences (Shanghai, China). HepG2 cells were cultured in RPMI-1640 medium supplemented with 10 % fetal bovine serum (FBS), 0.1 mg/mL streptomycin, and 100 U/mL penicillin at 37 ℃ in an atmosphere containing 5% carbon dioxide (CO_2). The compound 3-(4, 5-dimethylthiazol-2-yl)-2, 5-diphenyl tetrazolium bromide (MTT) was purchased from Dojindo Molecular Technologies, Inc. (Tokyo, Japan). Lipopolysaccharide (LPS), D-Hanks solution, RPMI-1640 medium, FBS and dimethyl sulfoxide (DMSO) were obtained from Gibco (Grand Island, NY, USA). Penicillin G and streptomycin were sourced from Sigma (Shanghai, China). All other chemicals and solvents utilized were of analytical grade, while CuB and CuE were synthesized in the laboratory of College of Pharmacy, Southwest Minzu University.

2.2 Cell viability assay 2.5×10^3 HepG2 cells/well were seeded in 96-well plates at a volume of 100 μL/well, and cultured for 24 h. The cells were subsequently incubated with different concentrations (0, 0.1, 1, 10, 100 μM) of cucurbitacin B and E for different periods (12, 24, 48, 72 h). At each time point, 10 μL of MTT reagent was added to the cells. After 4 h, the formazan crystals were solubilized overnight using a 10% sodium dodecyl sulfate solution. The results were quantified using a scanning multi-well spectrophotometer (Sunrise, RC, Tecan, Switzerland). All experiments were performed in triplicate, with three wells measured for each concentration in every replicate.

2.3 Flow cytometry analysis 10^6 HepG2 cells were seeded in six-well plates and were cultured for 24 h. Subsequently, the cells were treated with different concentrations of CuB and CuE (0, 0.1, 1, 10, 100 μM) for different periods. At the indicated time points, the cells were trypsinized and harvested, followed by a fixation with 70% ethanol at 4 ℃. Then, the cells were treated with 50 μg/mL RNase and stained with 25 μg/mL propidium iodide (PI) in the dark. The results were analyzed using the ModFit program (Becton Dickinson, USA).

Autophagy was evaluated with acridine orange (AO) staining, followed by analyses with flow cytometry and fluorescent microscopy[22]. Briefly, the cells were cultured in the absence or presence of glucose for either 12 or 24 h. Then, the cells were stained with 1 μM AO for 15 min at 37 ℃, after which the cells were trypsinized, washed, and collected in a phenol red-free growth medium. The fluorescence emission of green (510 – 530 nm) and red (650 nm) from cells illuminated with blue (488 nm) excitation light was measured using a flow cytometer. Depending on their acidity, autophagic lysosomes exhibited orange/red fluorescence, while cell nuclei displayed green fluorescence[22]. Autophagy was quantified as a ratio between geomean fluorescence intensity of red and green fluorescence (FL3/FL1). The data were presented as the fold changes, with arbitrarily setting of autophagy in cells without undergoing glucose deprivation as 1.

2.4 Western blot analysis HepG2 cells (10^6 cells/well) were seeded in six-well plates and treated with CuB and CuE as described earlier. At the indicated time points, the cell medium was removed, whereas the cells were washed, scraped in cold phosphate-buffered saline (PBS), and pelleted by centrifugation at 1 000 g for 5 min at 4 ℃. The cell pellet was re-suspended in lysis buffer, which was supplemented with protease and phosphatase inhibitors, and incubated for 1 h at 4 ℃. Subsequently, the lysate was centrifuged at 14 000 g for 40 min at 4 ℃, and the supernatant (total cell lysate) was collected and stored at −20 ℃. For Western blot analysis, 80 μg proteins were resolved over 10% polyacrylamide gel and subsequently transferred to a nitrocellulose membrane. The blot was incubated with blocking buffer composed of 5% non-fat dry milk/1 ‰ Tween-20 in Tris-buffered saline (TBS) for 1 h at room temperature. The proteins were stained overnight at 4 ℃ with appropriate primary antibodies in a blocking buffer, followed by incubation with horseradish peroxidase-conjugated secondary antibodies. The corresponding bands were visualized by enhanced chemiluminescence and autoradiography using X-ray film. GAPDH was used as a loading control.

2.5 RNA extraction, Illumina sequencing and data analysis HepG2 cells were seeded and treated as described above. Cells from different groups were harvested in Qiazol (QIAGEN Benelux B.V., Venlo, The Netherlands), after which the total RNA from each sample was isolated using TRIzol reagent (Invitrogen, Burlington, ON, Canada) according to the manufacturer's instructions. The concentration and quality of RNA were determined using a NanoPhotometer spectrophotometer (Implen, Inc., Westlake Village, CA, USA). The RNA integrity was determined by RNA 6000 Nano Assay kit. A total amount of 3 μg RNA per sample was used as the input material for the RNA sample preparations. Sequencing libraries were generated using NEBNext® Ultra™ RNA Library Prep Kit for Illumina®(NEB, USA) following manufacturer's recommendations, and index codes were added to attribute sequences to each sample. Transcriptome libraries were generated using the IlluminaTruSeq™ RNA Sample Preparation kit (Illumina, San Diego, CA, USA).

The transcriptomic data were analyzed using a previously described protocol with modifications[23]. Cleaned reads from each sample were mapped to a reference genome downloaded from a genomic database by TopHat v2.0.12. The gene expression levels were calculated using the FPKM method (fragments per kb per million reads)[24].

Differential expression genes (DEGs) analysis across different groups was performed by using the DESeq R package (version 1.18.0). DESeq provides statistical routines for determining differential expression via a model based on the negative binomial distribution. The resulting *P*-values were adjusted using the Benjamini and Hochberg's approach for controlling the false discovery rate. Genes with an adjusted *P*-value lower than 0.05 found by DESeq were considered as differentially expressed.

2.6 Function annotation Gene Ontology (GO) enrichment

analysis of differentially expressed genes was implemented by the GOseq R package, in which gene length bias was corrected. GO terms with corrected *P* value less than 0.05 were considered significantly enriched by DEGs. The Kyoto Encyclopedia of Genes and Genomes (KEGG) serves as a comprehensive database resource for understanding high-level functions and utilities of biological systems, including cells, organisms, and ecosystems, from molecular-level information, especially large-scale molecular datasets generated by genome sequencing and other high-throughput experimental technologies (http://www.genome.jp/kegg/). The KOBAS software was used to test the statistical enrichment of DEGs in KEGG pathways[25-26].

2.7 Statistical analysis Where appropriate, data were expressed as the mean ± standard error of the mean (SEM). A one-way analysis of variance (ANOVA) followed by a *t* test with GraphPad 7.0 was employed to compare the differences between individual groups. A two-sided *P*-value less than 0.05 was considered statistically significant.

3 Results and analysis

3.1 Anti-proliferation effect of CuB and CuE on HepG2 cell *in vitro* The viability of HepG2 cells treated with 0.1 to 100 μM of CuB and CuE for 12 to 72 h was measured with the MTT assay. As shown in Figs. 1-3, treatment with different concentrations of CuB and CuE resulted in a time- and dose-dependent inhibition of HepG2 cell proliferation. The cell proliferation was highest when incubated with different concentrations of CuB and CuE for 12 h, while the lowest viability was attained at 72 h. Furthermore, cell viability decreased with increasing concentrations of the compounds, with CuB and CuE at 100 μM showing the highest inhibition rate compared to other concentrations. In addition, CuB showed a more potent inhibitory effect on HepG2 cell growth than CuE.

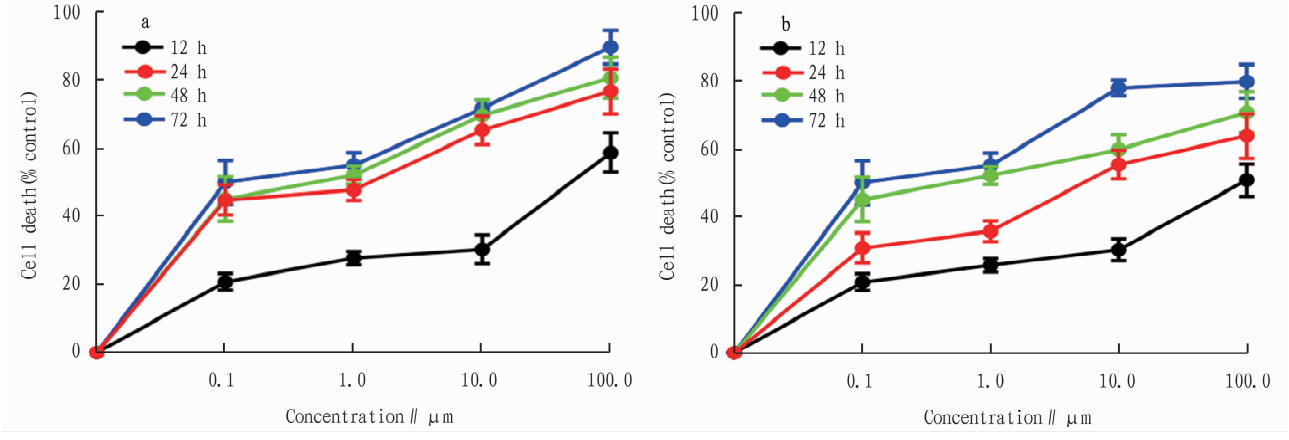

NOTE a: HepG2 cells were cultured with different concentration of CuB (0.1, 1, 10, 100 μM) for 12, 24, 48, and 72 h in RPMI 1640-10% FBS at 2.5×10^3 cells/well; b: HepG2 cells were cultured with different concentration of CuE (0.1, 1, 10, 100 μM) for 12, 24, 48, and 72 h in RPMI 1640-10% FBS at 2.5×10^3 cells/well. Each point represents the mean of the data from three independent experiments.

Fig. 1 Dose- and time-dependent anti-proliferation effect of CuB and CuE on the HepG2 cells

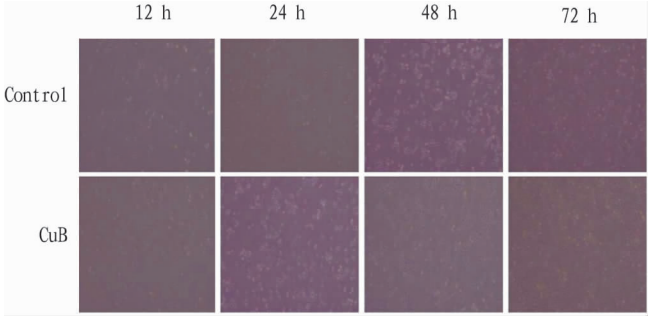

NOTE HepG2 cells were treated with solvent control or CuB (10 μM) at 12, 24, 48 and 72 h.

Fig. 2 Effect of CuB on HepG2 cell proliferation assay

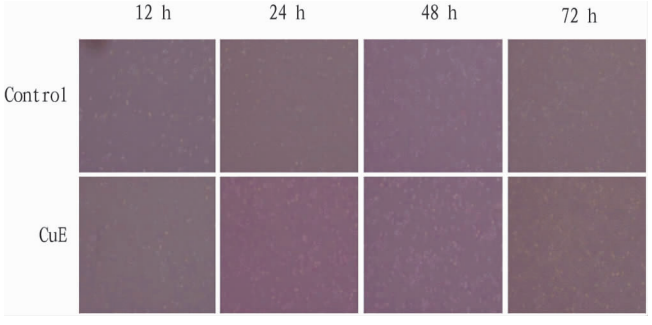

NOTE HepG2 cells were treated with solvent control or CuE (10 μM) at 12, 24, 48 and 72 h.

Fig. 3 Effect of CuE on HepG2 cell proliferation assay

3.2 Effect of CuB and CuE on HepG2 cell cycle and apoptosis To examine whether the cytotoxicity of CuB and CuE involves apoptosis, we investigated the expression of the activated fragment of cleaved caspase-3 using Western blot analysis. As shown in Fig. 4, the cleaved fragment of caspase-3 (35 kDa) was observed in the groups treated with CuB and CuE, indicating that both CuB and CuE could induce cell apoptosis, thus inhibiting the growth of HepG2 cells. We further determined the effect of the compounds on cell cycle distribution using flow cytometry. The percentages of cells in different cell phase (G_0/G_1, S and G_2/M) are presented

in Fig. 5. The results presented in Fig. 6 showed that treatment with CuB and CuE displayed moderate effects on the progression of cell cycle, as indicated by the similar number of cells in the G_2/M phase cells in all groups.

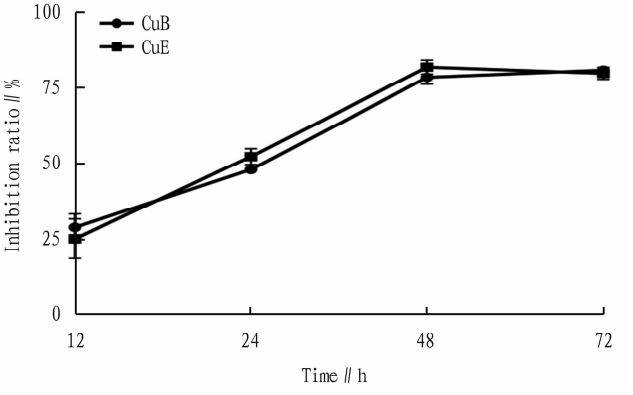

NOTE *OD* (450 nm) was determined by MTT assay at 12, 24, 48, and 72 h. The data represent the mean ± SE of three independent experiments.

Fig. 4 HepG2 cells cultured with CuB and CuE (10 μM) in CCK8 (10 μL CCK8/100 μL)

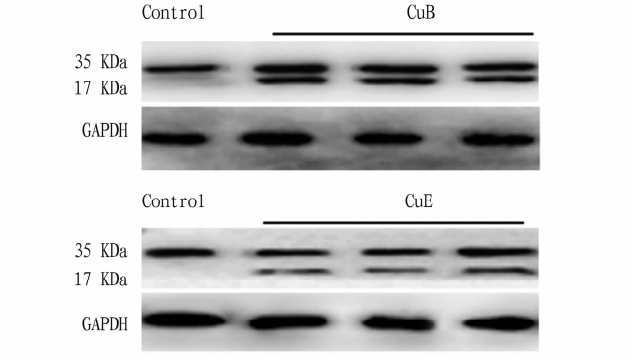

NOTE HepG2 cells were treated with 10 Mm CuB and CuE for 24 h. The cells were harvested and processed for Western blotting. GAPDH was used as the internal control. Immunoblot was a representative of three independent experiments.

Fig. 5 Western blot analysis of endogenous levels of full-length caspase-3 (35 kDa) and the large fragment of cleaved caspase-3 (17 kDa)

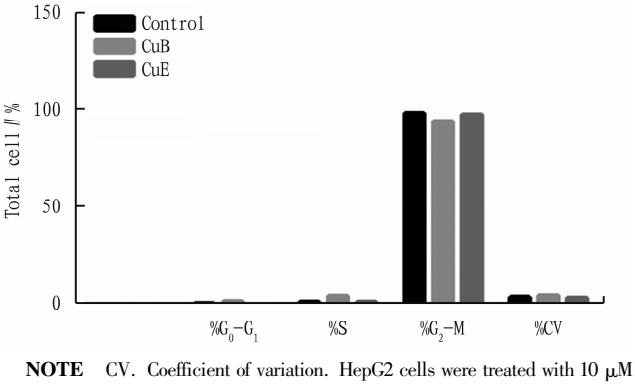

NOTE CV. Coefficient of variation. HepG2 cells were treated with 10 μM of CuB or CuE and analyzed using flow cytometry with PI staining.

Fig. 6 Effects of CuB and CuE on the distribution of HepG2 cell cycle phase (G_0/G_1, S and G_2/M)

3.3 Effect of CuB and CuE on HepG2 autophagy As CuB and CuE were shown to control the initiation of autophagy, we further assessed their effects on the inhibition of autophagy in HepG2 cells. After serum starvation, the cells were submitted to an AO staining to reveal AVOs, followed by analyses with fluorescence microscopy and fluorescence activated cell sorter (FACS) scanning. The data presented in Table 1 demonstrated that treatment with CuB and CuE showed a comparable number of autophagosomes when compared to the control group. Therefore, it can be concluded that CuB and CuE had no effect on HepG2 autophagy.

Table 1 Calculation of autophagy ratio in HepG2 cells after the treatment of CuB and CuE at various concentrations

Sample	Orange PE	Green FITC	Autophagy ratio (Orange PE/Green FITC)
CuB-1 // μmol/L	3 888.4	24 864.3	0.156
CuB-6 // μmol/L	3 541.7	20 068.7	0.176
CuB-12 // μmol/L	2 570.1	20 267.0	0.127
CuB-50 // μmol/L	7 053.2	31 848.8	0.221
Control-1	2 751.9	15 144.2	0.182
Control-2	3 037.7	23 066.8	0.132
CuE-3 // μmol/L	3 298.3	23 085.0	0.143
CuE-10 // μmol/L	3 778.4	19 217.5	0.197
CuE-25 // μmol/L	3 521.2	20 978.7	0.168

3.4 Transcriptome sequencing, de novo assembly and transcriptome profiles cDNA libraries of three groups were constructed and sequenced on an IlluminaHisSeq 2000 platform. After quality control, bands of a total size of 8.02G bp, 7.4G bp, 7.6G bp were obtained for control group, CuB- and CuE-treated groups, respectively. The detailed mapping results are shown in Table 2. The percentage of reads that were mapped to genomic regions and the FPKM density distribution of three groups are shown in Fig. 7. The abundance of genes was calculated and normalized through the use of uniquely mapped reads, employing the FPKM method. The distribution of gene expression levels in all groups was similar. Genes with FPKM values greater than 60 were classified as high expression genes, while those with FPKM values below one were considered as low expression or non-expression genes. The results showed that a total of 30 520 genes (52%) with FPKM values over 1 were detected in the control group. In the CuB and CuE treatment groups, 31 472 genes (approximately 53%) and 27 769 genes (approximately 47%) with FPKM values greater than 1 were detected, respectively. Furthermore, 2 432 genes (approximately 4.13 %) with FPKM vales exceeding 60 were found in the control group. In the CuB and CuE treatment groups, 2 349 genes (approximately 3.99%) and 2 279 genes (approximately 3.87%) with FPKM values greater than 60 were observed, respectively (Table 3). Moreover, seven genes (COX1, COX2, COX3, ND3, FTL, ND1 and APOA2) were extremely highly expressed (FPKM >5 000) in the control group, as illustrated in Table 4. In contrast, nine genes were extremely highly expressed in the CuB- and CuE-treated groups (COX1, COX2, COX3, ND3, FTL, ND1, APOA2, ATPase6 and ACTB).

Table 2 Summary of the mapping results

Sample name	Control	CuB	CuE
Total reads	50 855 214	45 603 310	54 313 582
Total mapped	48 187 797 (94.75%)	43 281 375 (94.91%)	51 448 086 (94.72%)
Multiple mapped	1 084 795 (2.13%)	1 005 856 (2.21%)	1 220 972 (2.25%)
Unique mapped	47 103 002 (92.62%)	42 275 519 (92.70%)	50 227 114 (92.48%)
Reads map to '+'	23 484 940 (46.18%)	21 070 827 (46.20%)	25 037 750 (46.10%)
Reads map to '−'	23 618 062 (46.44%)	21 204 692 (46.50%)	25 189 364 (46.38%)
Non-splice reads	28 718 045 (56.47%)	26 900 346 (58.99%)	32 438 927 (59.73%)
Splice reads	18 384 957 (36.15%)	15 375 173 (33.72%)	17 788 187 (32.75%)

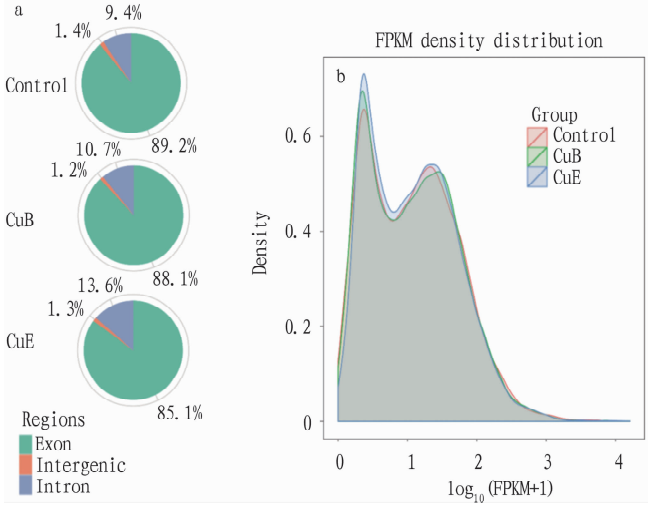

Fig. 7 Percentage of reads mapped to genome regions and the FPKM density distribution

Table 3 Summary of genes expression quantification summary

FPKM interval	Control	CuB	CuE
0 – 1	44 240 (75.08%)	44 430 (75.40%)	43 815 (74.36%)
1 – 3	3 172 (5.38%)	3 154 (5.35%)	3 541 (6.01%)
3 – 15	4 502 (7.64%)	4 359 (7.40%)	4 585 (7.78%)
15 – 60	4 576 (7.77%)	4 630 (7.86%)	4 702 (7.98%)
>60	2 432 (4.13%)	2 349 (3.99%)	2 279 (3.87%)

3.5 DEGs between the control versus CuB and CuE treated groups The clean reads were adjusted by the edgeR program with one scaling normalized factor. The DEGSeq R package was used to determine DEGs between the control group and the two treatment groups. Genes exhibiting a false discovery rate (FDR) lower than 0.01 and an absolute $\log_2$ fold change greater than 1 were considered as significant differential expression. In this study, hierarchical clustering analysis of DEGs was performed to identify the gene expression patterns based on the $\log_{10}$ padj of compound-treated groups versus control group, as illustrated in Fig. 8. In the CuB-

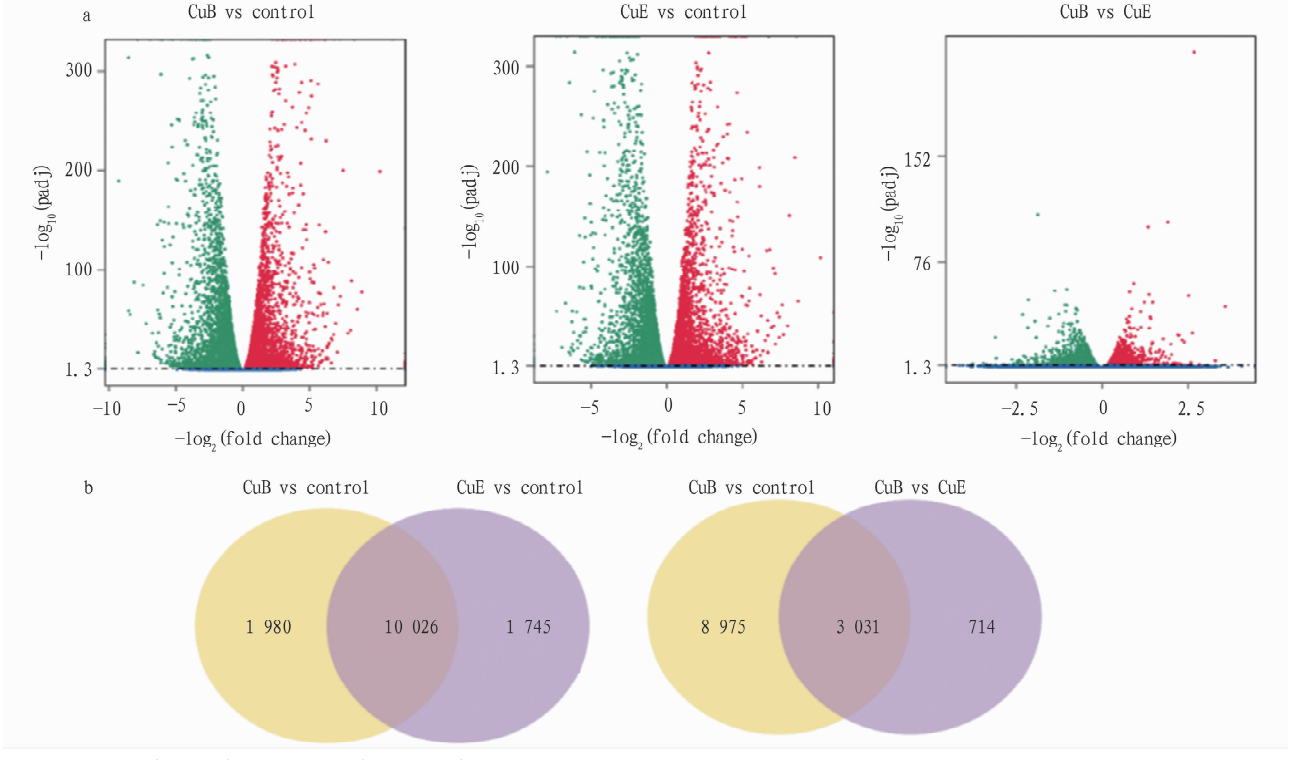

NOTE a. Volcano plot of DEGs; b. Venn diagram of DEGs.

Fig. 8 Summary of gene expression patterns

Table 4 Quantification of gene expression in different groups (FPKMs >5 000)

Gene ID	FPKM vlue			Symbol	Description	KEGG orthology
	Control	CuB	CuE			
198804	10 788.59	18 327.94	15 950.62	COX1	Cytochrome C Oxidase Subunit I	K02256
198712	10 694.64	14 405.14	12 556.51	COX2	Cytochrome C Oxidase Subunit II	K02261
198938	6 971.78	9 508.95	9 890.065	COX3	Cytochrome C Oxidase Subunit III	K02262
198840	6 493.89	8 676.25	7 816.26	ND3	NADH Dehydrogenase Subunit 3	K03880
87086	6 449.73	7 817.42	5 314.56	FTL	Ferritin, light polypeptide	K13625
198888	5 836.91	7 656.88	7 893.13	ND1	NADH Dehydrogenase Subunit 3	K03878
158874	5 217.73	1 309.16	1 270.72	APOA2	Apolipoprotein A-II	K08758
198899	4 834.46	5 673.18	5 383.12	ATPase6	Mitochondrial membrane ATP synthase subunit	K02126
75624	2 739.95	7 354.39	8 585.46	ACTB	Actin beta	K05692

treated group, a total of 12 006 unigenes were identified as DEGs, of which 5 880 were up-regulated and 6 126 were down-regulated. In the CuE-treated group, a total of 11 771 genes were identified as DEGs, including 5 722 up-regulated genes and 6 049 down-regulated genes. Comparing the DEGs between the CuB- and CuE-treated groups, a total of 10 026 genes were identified as DEGs in both groups. However, there were 3 745 DEGs between CuB- and CuE-treated groups. Several respective highly expressed DEGs, with an absolute $\log_2$ fold change greater than 7, are presented in Table 5. Among which SCN1A, FAM129A, TNFRSF9, TMEM71 and ADGRF4 were identified as extremely high expression DEGs in both the CuB- and CuE-treated groups.

Table 5 DEGs in the CuB and CuE treatment groups compared to the control group (absolute log2 fold change >7)

	Gene symbol	$\log_2$ Fold change	Description	KEGG orthology
CuB	*SCN1A*	-9.27	Sodium voltage-gated channel alpha subunit 1	K04833
	PLPPR1	-8.53	Phospholipid phosphatase related 1	K19581
	SERPINA12	-8.52	Serpin peptidase inhibitor, clade A	K04525
	MBL2	-8.11	Mannose binding lectin 2	K04141
	ACSM2B	-7.21	Acyl-CoA synthetase medium chain family member 2B	K01896
	FAM129A	10.26	Family with sequence similarity 129 member A	No assigned
	TMEM71	8.57	Transmembrane protein 71	No assigned
	RUFY4	8.14	RUN and FYVE domain containing 4	No assigned
	ADGRF4	7.89	Adhesion G protein-coupled receptor F4	K08457
	TNFRSF9	7.49	TNF receptor superfamily member 9	K05146
	C11orf96	7.08	Chromosome 11 open reading frame 96	No assigned
CuE	*SCN1A*	-7.86	Sodium voltage-gated channel alpha subunit 1	K04833
	UGT2B10	-7.85	UDP-glucuronosyl/UDP-glucosyltransferase	K00699
	CD14	-7	CD14 molecule	K04391
	FAM129A	10.15	Family with sequence similarity 129 member A	No assigned
	TNFRSF9	8.08	TNF receptor superfamily member 9	K05146
	TMEM71	7.98	Transmembrane protein 71	No assigned
	ADGRF4	7.64	Adhesion G protein-coupled receptor F4	K08457
	ACTC1	7.43	Actin, alpha, cardiac muscle 1	K12314
	RTP3	7.42	Receptor transporter protein 3	No assigned
	ACTA1	7.14	Actin, alpha 1, skeletal muscle	K10354

3.6 GO and KEGG enrichment analyses of the DEGs To explain the anti-tumor activity of CuB and CuE, GO and KEGG enrichment analyses of the DEGS were performed. After the treatment with CuB, the GO annotation yielded a total of 18 492 GO terms, which were categorized into biological processes (70.98%), molecular functions (20.13%) and cellular components (8.89%). After the treatment with CuE, a total of 18 479 GO terms were retrieved, including biological processes (71.12%), molecular functions (8.87%), and cellular components (20.01%). The network topology analysis of GO annotations indicated that the functions of DEGs were mainly distributed in several categories, such as "metabolic process" and "intracellular" (Fig.9). The results of KEGG pathway annotation of the CuB-treated group showed that 14 248 DEGs were enriched in 279 pathways, of which 21 pathways were significantly enriched ($P < 0.05$), including "spliceosome", "metabolic pathways", "cell cycle", and

"carbon metabolism" (Table 6 and Fig. 10). In comparison to the CuB-treated group, the annotation of the KEGG pathway of the CuE-treated group showed that 14 379 DEGs were enriched in 280 pathways, of which 15 pathways were significantly enriched, including "cell cycle", "spliceosome", "metabolic pathways", and "endocytosis" (Table 7 and Fig. 10). These results suggest that both CuB and CuE may regulate the gene expression in the same way related to metabolism and cellular growth.

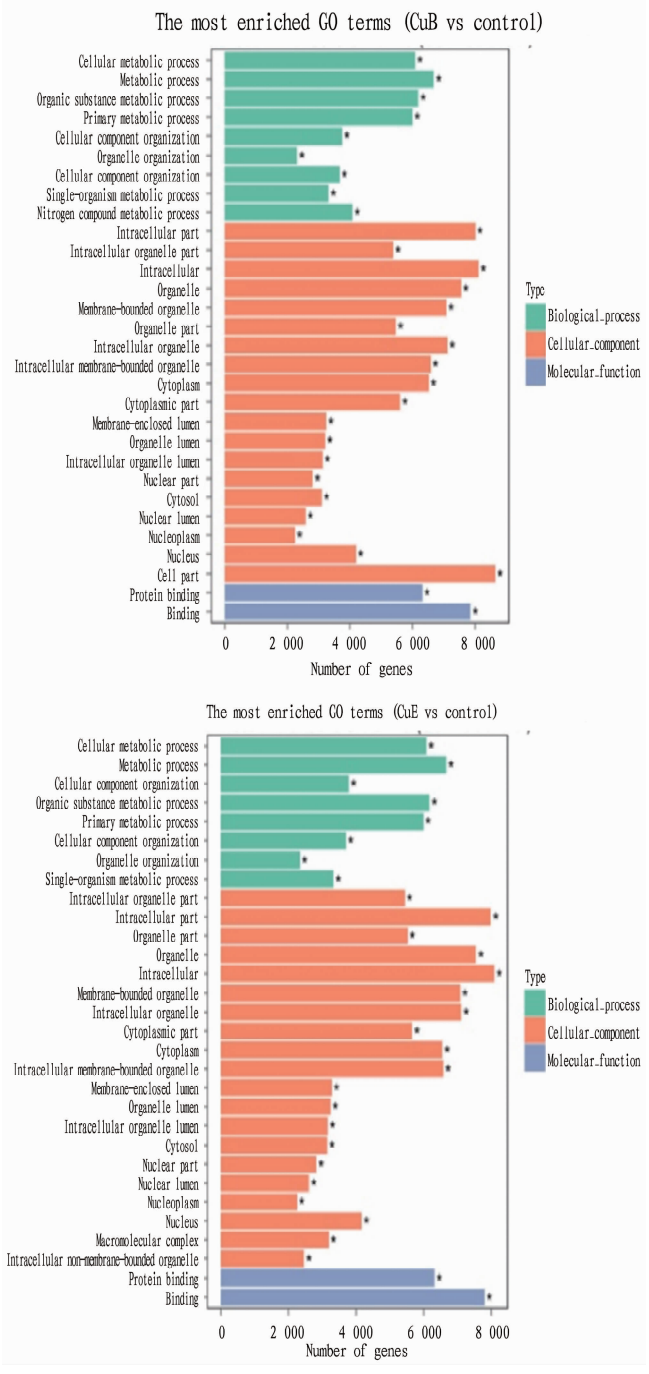

Fig. 9 GO annotation of DEGs

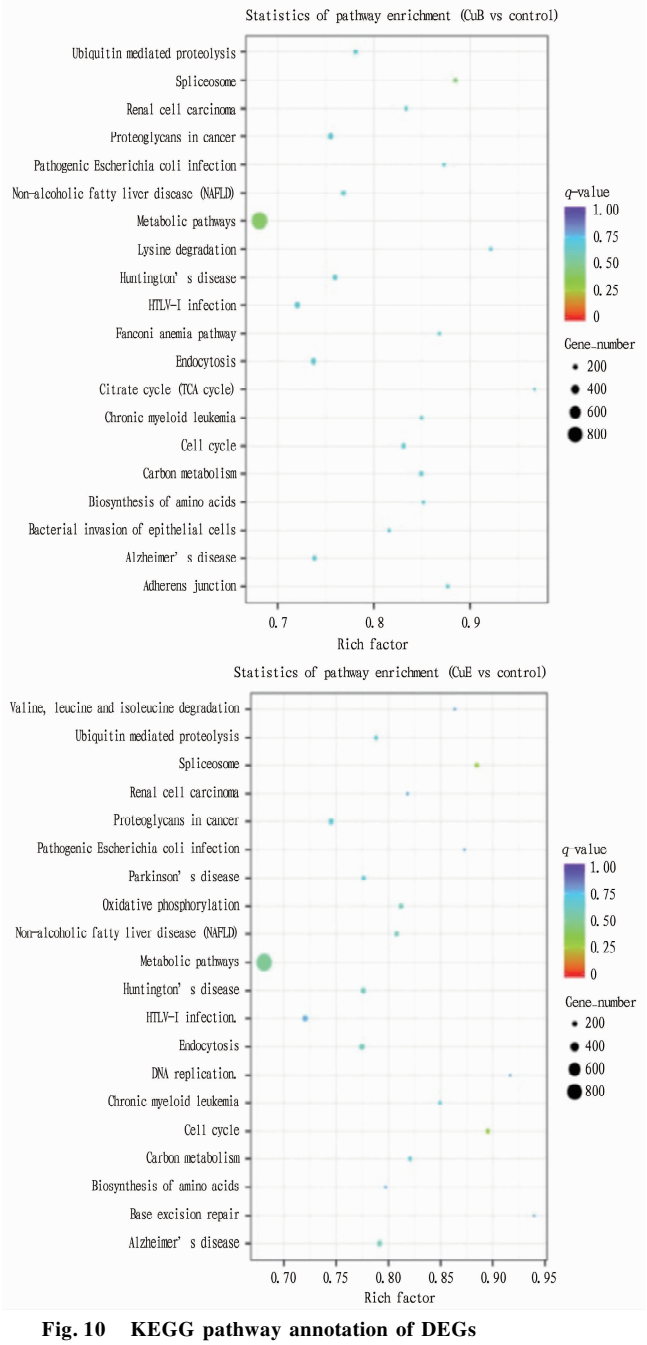

Fig. 10 KEGG pathway annotation of DEGs

Table 6 KEGG pathway annotation of DEGs after CuB treatment

Term	DEGs with pathway annotation (14 248)	*P*-value
Spliceosome	115 (0.81%)	0.001 697 251
Metabolic pathways	826 (5.78%)	0.002 909 634
Cell cycle	103 (0.72%)	0.009 719 306
Carbon metabolism	90 (0.63%)	0.010 282 907
Adherens junction	64 (0.45%)	0.017 900 414
Proteoglycans in cancer	154 (1.08%)	0.019 700 975
Huntington's disease	139 (0.98%)	0.022 604 697

(To be continued)

(Continued)

Term	DEGs with pathway annotation (14 248)	*P*-value
Lysine degradation	47 (0.33%)	0.022 963 425
Ubiquitin mediated proteolysis	107 (0.75%)	0.025 899 529
Biosynthesis of amino acids	63 (0.44%)	0.027 031 516
Non-alcoholic fatty liver disease (NAFLD)	116 (0.81%)	0.028 385 971
Chronic myeloid leukemia	62 (0.44%)	0.028 914 261
Endocytosis	157 (1.10%)	0.030 990 975
HTLV-I infection	188 (1.32%)	0.034 083 770
Pathogenic Escherichia coli infection	48 (0.34%)	0.038 108 327
Fanconi anemia pathway	46 (0.32%)	0.043 917 894
Citrate cycle (TCA cycle)	29 (0.20%)	0.046 098 972
Bacterial invasion of epithelial cells	62 (0.44%)	0.046 270 585
Renal cell carcinoma	55 (0.37%)	0.046 309 958
Alzheimer's disease	124 (0.87%)	0.048 828 131
Base excision repair	31 (0.22%)	0.049 605 022

Table 7 KEGG pathway annotation of DEGs after CuE treatment

Term	DEGs with pathway annotation (14 379)	*P*-value
Cell cycle	111 (0.77%)	0.001 948 100
Spliceosome	115 (0.80%)	0.002 140 578
Metabolic pathways	826 (5.74%)	0.005 478 063
Endocytosis	165 (1.15%)	0.011 263 733
Non-alcoholic fatty liver disease (NAFLD)	122 (85.00%)	0.011 632 188
Alzheimer's disease	133 (0.92%)	0.013 494 029
Oxidative phosphorylation	108 (0.75%)	0.015 262 775
Huntington's disease	142 (0.99%)	0.016 927 700
Carbon metabolism	87 (0.61%)	0.022 987 456
Ubiquitin mediated proteolysis	108 (0.75%)	0.025 622 131
Parkinson's disease	111 (0.77%)	0.031 174 852
Chronic myeloid leukemia	62 (0.43%)	0.032 663 604
Proteoglycans in cancer	152 (1.06%)	0.032 667 923
Pathogenic Escherichia coli infection	48 (0.33%)	0.042 184 084
HTLV-I infection	188 (1.31%)	0.042 207 042

4 Discussion

CuB and CuE are compounds that belong to the cucurbitacin family and have been isolated from various plant sources[27-28]. Previous evidences have demonstrated that CuB and CuE exhibit inhibitory activities against numerous human cancer cells[29-32]. In the present study, we studied the inhibitory effects of CuB and CuE on HepG2 cells. The results indicated that CuB and CuE showed an inhibitory effect on the growth of HepG2 cell lines in a dose- and time- dependent manner, as demonstrated by the MTT assay. CuB and CuE treatment inhibited cell growth with IC_{50} value of 10 μM for the HepG2 cell line after 24 h. To the best of our knowledge, this study represents the first comparative analysis of the anti-tumor effects of CuB and CuE on the HepG2 cell line.

Most anti-cancer agents exhibit their inhibitory effects on tumor cell growth by inducing cell cycle arrest and apoptosis. Previous reports have demonstrated that CuB and CuE induce G_2/M arrest and apoptosis in human laryngeal squamous cell lines[10] and in human breast cancer cell lines[33]. To determine the potential of CuB and CuE to induce cell cycle arrest and apoptosis in the HepG2 cell line, we performed a cell cycle analysis. The results showed that both CuB and CuE were able to induce cell cycle arrest at the G_2/M phase.

To better understand the potential mechanism by which CuB and CuE induce cell cycle arrest and apoptosis in HepG2 cells, we further investigated the status of key proteins known to regulate apoptosis. Our findings clearly demonstrated that the levels of full-length caspase-3 (35 kDa) and the large fragment of cleaved caspase-3 (17 kDa) were increased in HepG2 cells treated with either CuB or CuE. This suggested that CuB and CuE could activate the caspase activity of HepG2 cells, thereby initiating an apoptotic program. In addition, the changes in the CuB-treated group were greater than those in the CuE-treated group. These results explained the anti-proliferation role of CuB and CuE on HepG2 cells.

Autophagy plays an important role in cancer. It functions as a tumor suppressor in certain scenarios[34-37], while simultaneously acting as a tumor promoter in others[38-40]. Tumor cells often activate autophagy in response to cellular stress and/or increased metabolic demands related to rapid cell proliferation. Targeting autophagy in cancer will provide novel opportunities for drug development, as there is a pressing need for more potent and specific inhibitors of autophagy. However, our data showed that CuB and CuE had no effect on autophagy in HepG2 cells. This means that the anti-tumor role of CuB and CuE did not occur via the induction of autophagy in HepG2 cells.

Recently, several studies have indicated that different cucurbitacin species exhibit distinct biological activities against tumor expansion. For instance, CuB, cucurbitacin I (CuI), and cucurbitacin Q (CuQ) have been shown to specifically inhibit the phosphorylation of signal transducer and activator of transcription 3 (STAT3), a process that contributes to the proliferation of numerous cancerous cells[30, 41-43]. Besides, CuB could inhibit the translational expression of hypoxia-inducible factor-1, leading to a decreased growth of HeLa cells in a xenograft tumor model[44]. Additionally, the previous study showed that CuE induced caspase-dependent apoptosis and protective autophagy mediated by reactive oxygen species (ROS) in 95D lung cancer cells[45]. Although the anti-cancer activities of CuB and CuE in certain cell types have been reported, the underlying molecular mechanisms responsible for these activities were poorly understood. Therefore, a combined evaluation of gene expression alterations and relevant functional endpoints using HepG2 cells may contribute to a better understanding of the modes of action of CuB and CuE and their anti-tumor activities. In the current study, we found that several genes were extremely highly expressed after treatment with CuB and CuE in comparison to the control group. Cytochrome coxidase (COX) is com-

posed of 13 subunits, of which COX2 has been implicated in some tumor cells, and numerous studies are currently focused on the discovery of COX2 specific inhibitors[46]. Here, mRNA-sequencing results showed that COX2 was highly expressed in HepG2 cells. Notably, CuB and CuE showed no inhibition on the expression of this gene. Interestingly, the FPKMs of the Actin beta (*ACTB*) gene were recorded as 7 354.39 and 8 585.46 in the CuB- and CuE-treated groups, whereas the FPKM value of the *ACTB* was 2 739.95 in the control group. ACTB are highly conserved proteins that are involved in cell motility, structure and integrity. Changes of ACTB may associate with the cell morphology[47-48]. In this study, our results showed that CuB and CuE could up-regulate the expression of ACTB, thus affecting cell morphology. The voltage-gated sodium channel gene *SCN1A* expressed in HepG2 cells played roles in the generation of action potentials and the maintenance of cellular homeostasis. The down-regulated expression of *SCN1A* in the CuB- and CuE-treated groups demonstrated that this gene might be responsible for maintaining the viability of HepG2 cells. The up-regulated gene *FAM129A* functions as an inhibitor of cell growth. *TNFRSF9* encodes a cytokine that is a member of the tumor necrosis factor (TNF) ligand family. This cytokine is involved in the process of antigen presentation and the generation of cytotoxic T cells. Additionally, *TMEM71* and *ADGRF4* are considered to be responsible for the G-protein coupled receptor activity and transmembrane signaling receptor activity.

The function analysis of DEGs was implemented by the GOseq R package. This revealed DEGs related to "metabolic process" and "cellular metabolic process". These metabolism-related pathways or processes seemed to be down-regulated by CuB and CuE. In accordance with the results of GO annotation, KEGG annotation of DEGS also showed that CuB and CuE may interfere with several biological processes, including "metabolic pathways", "spliceosome", "cell cycle", and "carbon metabolism". In our research, we observed that the cell cycle pathway was inhibited by CuB and CuE, which play critical roles in cell proliferation. These results suggest that CuB and CuE may attack cancer cells through multiple pathways, including the cell cycle, and might be more effective than specific inhibitors. In addition, cancer cells have high metabolic demands due to increased cellular proliferation. In in vivo models, exposure to metabolic stress was shown to impair the survival of autophagy-deficient cells compared to autophagy-proficient cells[36]. The KEGG pathways annotation of DEGs after CuE and CuB treatment showed that the inhibition of the metabolic pathways can enhance tumor cell death through diverse anti-cancer therapies.

Despite the tremendous amount of research that remains uncompleted, it is evident that signal transduction pathways interact to regulate cell cycle progression and apoptosis. An understanding of how CuB and CuE control the expression of cell cycle regulatory genes through transcriptional mechanisms may reveal novel strategies to prevent their aberrant activation in HepG2 cells. More research in metabolomics is necessary to indentify clear cellular and molecular targets for the treatment of human hepatocellular carcinoma.

5 Conclusions

In conclusion, we found that the anti-tumor effects of CuB and CuE on HepG2 cells were due to the induction of cell cycle arrest and apoptosis. In addition, we demonstrated that CuB and CuE have little effect on gene expression patterns of HepG2 cells, although there was minor difference in the gene expression of CuB- and CuE-treated HepG2 cells. These results suggest a potential clinical application of CuB and CuE in the treatment of hepatocellular carcinoma.

References

[1] FORNER A, RODRÍGUEZ - LOPEZ C, REIG M. Natural history and staging for hepatocellular carcinoma[J]. Clinical Liver Disease, 2012, 1(6): 183-185.

[2] DAVILA JA, DUAN Z, MCGLYNN KA, *et al.* Utilization and outcomes of palliative therapy for hepatocellular carcinoma: A population-based study in the United States[J]. Journal of Clinical Gastroenterology, 2012, 46(1): 71-77.

[3] BRUIX J, SHERMAN M. Management of hepatocellular carcinoma: An update[J]. Hepatology, 2011, 53(3): 1020-1022.

[4] LLOVET JM, RICCI S, MAZZAFERRO V, *et al.* Sorafenib in advanced hepatocellular carcinoma[J]. New England Journal of Medicine, 2008, 359(4): 378-390.

[5] SPORN MB, SUH N. Chemoprevention of cancer[J]. Carcinogenesis, 2000, 21(3): 525-530.

[6] CHEN JC, CHIU MH, NIE RL, *et al.* Cucurbitacins and cucurbitane glycosides: Structures and biological activities[J]. Natural Product Reports, 2005, 22(3): 386-399.

[7] CAI Y, FANG X, HE C, *et al.* Cucurbitacins: A systematic review of the phytochemistry and anticancer activity[J]. The American Journal of Chinese Medicine, 2015, 43(7): 1331-1350.

[8] LEE DH, IWANSKI GB, THOENNISSEN NH. Cucurbitacin: Ancient compound shedding new light on cancer treatment[J]. The Scientific World Journal, 2010, 10: 413-418.

[9] JAYAPRAKASAM B, SEERAM NP, NAIR MG. Anticancer and antiinflammatory activities of cucurbitacins from Cucurbita andreana[J]. Cancer Letters, 2003, 189(1): 11-16.

[10] LIU T, ZHANG M, ZHANG H, *et al.* Inhibitory effects of cucurbitacin B on laryngeal squamous cell carcinoma[J]. European Archives of Oto-rhino-laryngology, 2008, 265(10): 1225-1232.

[11] TANNIN-SPITZ T, GROSSMAN S, DOVRAT S, *et al.* Growth inhibitory activity of cucurbitacin glucosides isolated from Citrullus colocynthis on human breast cancer cells[J]. Biochemical Pharmacology, 2007, 73(1): 56-67.

[12] HUNG CM, CHANG CC, LIN CW, *et al.* Cucurbitacin E as inducer of cell death and apoptosis in human oral squamous cell carcinoma cell line SAS[J]. International Journal of Molecular Sciences, 2013, 14(8): 17147-17156.

[13] ZHA QB, ZHANG XY, LIN QR, *et al.* Cucurbitacin E induces autophagy via downregulating mTORC1 signaling and upregulating AMPK activity[J]. PLoS One, 2015, 10(5): e0124355.

[14] KUO TCY, CHEN CH, CHEN SH, *et al.* The effect of red light and far-red light conditions on secondary metabolism in agarwood[J]. BMC Plant Biology, 2015, 15(1): 139-148.

[15] GUO L, DIAL S, SHI L, *et al.* Similarities and differences in the ex-

pression of drug-metabolizing enzymes between human hepatic cell lines and primary human hepatocytes[J]. Drug Metabolism and Disposition, 2011, 39(3): 528 – 538.
[16] KNASMÜLLER S, MERSCH-SUNDERMANN V, KEKEVORDES S, *et al.* Use of human-derived liver cell lines for the detection of environmental and dietary genotoxicants; current state of knowledge[J]. Toxicology, 2004, 198(1 – 3): 315 – 328.
[17] DVORÁK Z, VRZAL R, ŠTARHA P, *et al.* Effects of dinuclear copper (II) complexes with 6-(benzylamino) purine derivatives on AhR and PXR dependent expression of cytochromes P450 CYP1A2 and CYP3A4 genes in primary cultures of human hepatocytes[J]. Toxicology in Vitro, 2010, 24(2): 425 – 429.
[18] CHEN Y, HUANG C, ZHOU T, *et al.* Genistein induction of human sulfotransferases in HepG2 and Caco-2 cells[J]. Basic & Clinical Pharmacology & Toxicology, 2008, 103(6): 553 – 559.
[19] LIGUORI MJ, BLOMME EA, WARING JF. Trovafloxacin-induced gene expression changes in liver-derived *in vitro* systems: Comparison of primary human hepatocytes to HepG2 cells[J]. Drug Metabolism and Disposition, 2008, 36(2): 223 – 233.
[20] LANÇON A, HANET N, JANNIN B, *et al.* Resveratrol in human hepatoma HepG2 cells: Metabolism and inducibility of detoxifying enzymes [J]. Drug Metabolism and Disposition, 2007, 35(5): 699 – 703.
[21] JENNEN DG, GAJ S, GIESBERTZ PJ, *et al.* Biotransformation pathway maps in WikiPathways enable direct visualization of drug metabolism related expression changes[J]. Drug Discovery Today, 2010, 15(19 – 20): 851 – 858.
[22] VUCICEVIC L, MISIRKIC M, KRISTINA J, *et al.* Compound C induces protective autophagy in cancer cells through AMPK inhibition-independent blockade of Akt/mTOR pathway[J]. Autophagy, 2011, 7(1): 40 – 50.
[23] SUN Q, ZHOU G, CAI Y, *et al.* Transcriptome analysis of stem development in the tumourous stem mustard *Brassica juncea* var. *tumida* Tsen et Lee by RNA sequencing[J]. BMC Plant Biology, 2012, 12(1): 53 – 62.
[24] HART SN, THERNAU TM, ZHANG Y, *et al.* Calculating sample size estimates for RNA sequencing data[J]. Journal of Computational Biology, 2013, 20(12): 970 – 978.
[25] KANEHISA M, FURUMICHI M, TANABE M, *et al.* KEGG: New perspectives on genomes, pathways, diseases and drugs[J]. Nucleic Acids Research, 2016, 45(D1): D353 – D361.
[26] WALLER LP, DESHPANDE V, PYRSOPOULOS N. Hepatocellular carcinoma: A comprehensive review[J]. World Journal of Hepatology, 2015, 7(26): 2648 – 2663.
[27] ALGHASHAM AA. Cucurbitacins: A promising target for cancer therapy [J]. International Journal of Health Sciences, 2013, 7(1): 77 – 89.
[28] SHANG Y, MA Y, ZHOU Y, *et al.* Biosynthesis, regulation, and domestication of bitterness in cucumber[J]. Science, 2014, 346(6213): 1084 – 1088.
[29] LIU T, ZHANG M, DENG Y, *et al.* Effects of cucurbitacin B on cell proliferation and apoptosis in Hep-2 cells[J]. Journal of Clinical Otorhinolaryngology, Head, and Neck Surgery, 2008, 22(9): 403 – 407.
[30] LIU T, PENG H, ZHANG M, *et al.* Cucurbitacin B, a small molecule inhibitor of the Stat3 signaling pathway, enhances the chemosensitivity of laryngeal squamous cell carcinoma cells to cisplatin[J]. European Journal of Pharmacology, 2010, 641(1): 15 – 22.
[31] DONG Y, LU B, ZHANG X, *et al.* Cucurbitacin E, a tetracyclic triterpenes compound from Chinese medicine, inhibits tumor angiogenesis through VEGFR2-mediated Jak2-STAT3 signaling pathway[J]. Carcinogenesis, 2010, 31(12): 2097 – 2104.
[32] ZHANG M, BIAN Z-G, ZHANG Y, *et al.* Cucurbitacin B inhibits proliferation and induces apoptosis via STAT3 pathway inhibition in A549 lung cancer cells[J]. Molecular Medicine Reports, 2014, 10(6): 2905 – 2911.
[33] LAN T, WANG L, XU Q, *et al.* Growth inhibitory effect of cucurbitacin E on breast cancer cells[J]. International Journal of Clinical and Experimental Pathology, 2013, 6(9): 1799 – 1805.
[34] QU X, YU J, BHAGAT G, *et al.* Promotion of tumorigenesis by heterozygous disruption of the beclin 1 autophagy gene[J]. The Journal of Clinical Investigation, 2003, 112(12): 1809 – 1820.
[35] CHEN N, DEBNATH J. Autophagy and tumorigenesis[J]. FEBS Letters, 2010, 584(7): 1427 – 1435.
[36] MATHEW R, KARP CM, BEAUDOIN B, *et al.* Autophagy suppresses tumorigenesis through elimination of p62[J]. Cell, 2009, 137(6): 1062 – 1075.
[37] YOUNG AR, NARITA M, FERREIRA M, *et al.* Autophagy mediates the mitotic senescence transition[J]. Genes & Development, 2009, 23(7): 798 – 803.
[38] YOO BH, WU X, DEROUET M, *et al.* Hypoxia-induced downregulation of autophagy mediator Beclin-1 reduces the susceptibility of malignant intestinal epithelial cells to hypoxia-dependent apoptosis[J]. Autophagy, 2009, 5(8): 1166 – 1179.
[39] TURCOTTE S, CHAN DA, SUTPHIN PD, *et al.* A molecule targeting VHL-deficient renal cell carcinoma that induces autophagy[J]. Cancer Cell, 2008, 14(1): 90 – 102.
[40] FUNG C, LOCK R, GAO S, *et al.* Induction of autophagy during extracellular matrix detachment promotes cell survival[J]. Molecular Biology of the Cell, 2008, 19(3): 797 – 806.
[41] SUN J, BLASKOVICH MA, JOVE R, *et al.* Cucurbitacin Q: A selective STAT3 activation inhibitor with potent antitumor activity[J]. Oncogene, 2005, 24(20): 3236 – 3245.
[42] BLASKOVICH MA, SUN J, CANTOR A, *et al.* Discovery of JSI-124 (cucurbitacin I), a selective Janus kinase/signal transducer and activator of transcription 3 signaling pathway inhibitor with potent antitumor activity against human and murine cancer cells in mice[J]. Cancer Research, 2003, 63(6): 1270 – 1279.
[43] ZHANG M, SUN C, SHAN X, *et al.* Inhibition of pancreatic cancer cell growth by cucurbitacin B through modulation of signal transducer and activator of transcription 3 signaling[J]. Pancreas, 2010, 39(6): 923 – 929.
[44] MA J, JIANG YZ, SHI H, *et al.* Cucurbitacin B inhibits the translational expression of hypoxia-inducible factor-1α[J]. European Journal of Pharmacology, 2014, 723: 46 – 54.
[45] MA G, LUO W, LU J, *et al.* Cucurbitacin E induces caspase-dependent apoptosis and protective autophagy mediated by ROS in lung cancer cells [J]. Chemico-Biological Interactions, 2016, 253: 1 – 9.
[46] SILVA PJ, FERNANDES PA, RAMOS MJ. A theoretical study of radical-only and combined radical/carbocationic mechanisms of arachidonic acid cyclooxygenation by prostaglandin H synthase [J]. Theoretical Chemistry Accounts, 2003, 110(5): 345 – 351.
[47] ZHANG M, ZHANG H, SUN C, *et al.* Targeted constitutive activation of signal transducer and activator of transcription 3 in human hepatocellular carcinoma cells by cucurbitacin B[J]. Cancer Chemotherapy and Pharmacology, 2009, 63(4): 635 – 642.
[48] PECKHAM M, MILLER G, WELLS C, *et al.* Specific changes to the mechanism of cell locomotion induced by overexpression of (β)-actin [J]. Journal of Cell Science, 2001, 114(7): 1367 – 1377.